Replication of a Cytopathic Strain of Bovine Viral Diarrhea Virus Activates PERK and Induces Endoplasmic Reticulum Stress-Mediated Apoptosis of MDBK Cells

Robert Jordan, Lijuan Wang, Thomas M. Graczyk, Timothy M. Block, and Patrick R. Romano*

Department of Biochemistry and Molecular Pharmacology, The Jefferson Center for Biomedical Research, Thomas Jefferson University, Doylestown, Pennsylvania 18901

Endoplasmic reticulum (ER) stress signaling is an adaptive cellular response to the loss of ER Ca^{2+} homeostasis and/or the accumulation of misfolded, unassembled, or aggregated proteins in the ER lumen. ER stress-activated signaling pathways regulate protein synthesis initiation and can also trigger apoptosis through the ER-associated caspase 12. Viruses that utilize the host cell ER as an integral part of their life cycle would be predicted to cause some level of ER stress. Bovine viral diarrhea virus (BVDV) is a positive-stranded RNA virus of the *Flaviviridae* family. BVDV and related flaviviruses use the host ER as the primary site of envelope glycoprotein biogenesis, genomic replication, and particle assembly. We are using a cytopathic strain of BVDV (cpBVDV) that causes cellular apoptosis as a model system to determine how virus-induced ER stress contributes to pathogenesis. We show that, in a natural infection of MDBK cells, cpBVDV activates the ER transmembrane kinase PERK (PKR-like ER kinase) and causes hyperphosphorylation of the translation initiation factor eIF2α, consistent with the induction of an ER stress response. Additionally, we show that initiation of cellular apoptosis correlates with downregulation of the antiapoptotic Bcl-2 protein, induced expression of caspase 12, and a decrease in intracellular glutathione levels. Defining the molecular stress pathways leading to cpBVDV-induced apoptosis provides the basis to study how other ER-tropic viruses, such as hepatitis C and B viruses, modulate the host cell ER stress response during the course of persistent infection.

The endoplasmic reticulum (ER) regulates cellular metabolism and protein synthesis in response to perturbations in protein folding and biosynthesis (27). Physiologic or drug-induced disruption of protein folding causes misfolded, aggregated, or unassembled proteins to accumulate in the lumen of the ER, triggering an ER stress response (22). The ER stress response works at the level of protein translation and appears to be graded to the level of stress; mild ER stress modulates protein synthesis initiation and can slow cell growth, while extreme or prolonged ER stress can lead to apoptosis mediated by the ER-associated caspase 12 (see Fig. 8) (22).

The ER transmembrane kinase PERK (PKR-like ER kinase) couples ER stress signaling to changes in cellular metabolism (16, 17). PERK is activated in response to unfolded proteins in the ER lumen and downregulates protein translation through phosphorylation of eukaryotic initiation factor 2 (eIF2α) (26, 40). PERK-mediated eIF2α phosphorylation correlates with transcriptional induction of the ER chaperone GRP78 and the transcription factor *CHOP/GADD153* (40). Overexpression of GRP78 delays the onset of apoptosis induced by unfolded proteins, while overexpression of *CHOP/GADD153* leads to transcriptional downregulation of the antiapoptotic *bcl-2* gene and promotes apoptosis (11, 12, 31, 55). Thus, ER stress induces both pro- and antiapoptotic signaling,

with the fate of the cell possibly determined by the strength and duration of PERK-mediated ER stress signaling.

ER stress-induced downregulation of Bcl-2 expression leads to depletion of intracellular glutathione (GSH) and increased levels of reactive oxygen species (ROS) (28). These changes in intracellular redox status may contribute to activating the apoptotic program. A recently identified cysteine protease, caspase 12, is a key mediator of ER stress-induced apoptosis (33, 36, 54). Caspase 12 is associated with the cytoplasmic face of the ER and cleaved to an active form by caspase 7 in response to prolonged ER stress (36). The molecular mechanisms leading from ER stress signaling to caspase 12 activation are not known, but recent work has shown that, once activated, caspase 12 can recruit other cytosolic caspases to the ER membrane and that this caspase clustering may be a way to propagate the apoptotic signal (36).

Viruses that use the ER as an integral part of their replication strategy must contend with the ER stress response and the downstream consequences of ER stress signaling. Bovine viral diarrhea virus (BVDV) is an ER-tropic virus that belongs to the *Flaviviridae* family. This virus family encompasses important human pathogens such as hepatitis C virus (HCV), West Nile virus, Japanese encephalitis virus, dengue virus, and yellow fever virus. BVDV and related flaviviruses utilize the ER as the primary site of polyprotein processing, envelope glycoprotein biogenesis, and virion formation (20, 32, 44, 51, 52). Two biotypes of BVDV exist that can be distinguished phenotypically by their ability to cause cytopathic effects (30). Cytopathic strains of BVDV (cpBVDV) cause accumulation of

* Corresponding author. Mailing address: Department of Biochemistry and Molecular Pharmacology, The Jefferson Center for Biomedical Research, Thomas Jefferson University, Doylestown, PA 18901. Phone: (215) 489-4911. Fax: (215) 489-4920. E-mail: Patrick.Romano @mail.tju.edu.

ROS and induce apoptosis of the infected cell (18, 41, 56). While infection with cpBVDV results in cellular apoptosis, the virus-induced signals that initiate the apoptotic program have not been identified.

In this report, we show that cpBVDV activates ER stress signaling pathways that contribute to apoptosis of infected cells. Northern and immunoblot analyses were used to monitor expression of ER stress marker gene products during BVDV infection. We demonstrate that infection of MDBK cells with cpBVDV strain NADL induces GRP78 expression, PERK phosphorylation, and an increase in eIF2α phosphorylation. Infection with cpBVDV also induces *CHOP/GADD153* expression and downregulates Bcl-2 protein levels. Infected cells become depleted for intracellular GSH through a virus-induced mechanism that decreases transcription of glutamate cysteine ligase (GCL), the rate-limiting enzyme in GSH biosynthesis. Finally, cpBVDV infection induces caspase 12 expression. These results define a cellular cpBVDV-induced ER stress response that results in caspase activation and apoptosis. The ability of BVDV and other ER-tropic viruses to regulate the ER stress response pathway may dictate the fate of the infected cell and determine whether these viruses produce cytopathic effects or replicate noncytolytically to establish persistent infections.

MATERIALS AND METHODS

Cell culture, viruses, and plasmids. Madin-Darby bovine kidney (MDBK; ATCC-CCL22) cells were grown in Dulbecco's modified Eagle's medium/F12 medium supplemented with 10% heat-inactivated horse serum (Gibco-BRL, Gaithersburg, Md.). MDBK cells were tested for BVDV contamination by reverse transcription (RT)-PCR as described previously (46). The cytopathic NADL strain of BVDV was kindly provided by Ruben Donis, University of Nebraska, and was prepared by transfection of infectious RNA transcribed in vitro from an infectious cDNA clone (49). The resulting virus stock was plaque purified three times on MDBK cell monolayers prior to large-scale virus stock preparation.

Plasmid DNA containing cDNA inserts for selected ER stress-responsive genes was used to prepare radiolabeled probes for Northern hybridizations. The plasmid containing the *CHOP/GADD153* cDNA (GenBank accession number BE478941) was obtained from an expressed sequence tag library (BacPac Resources, Oakland, Calif.). The plasmid containing the full-length bovine GRP78 cDNA was cloned from an MDBK cDNA library (Clontech, Inc., Palo Alto, Calif.). The plasmid containing the human GCLC cDNA was kindly provided by R. Timothy Mulcahy (Department of Pharmacology, University of Wisconsin Medical School). Bovine actin cDNA was isolated by RT-PCR amplification of bovine actin RNA from MDBK cells.

Primers 5'-GTCTTCCCCTCCATTGTG-3' and 5'-CGGAACCGCTCATTG CTG-3' were designed based on the sequence for bovine β-actin (GenBank accession number UO2295). RT-PCR was performed with the Titan 1 RT-PCR kit according to the manufacturer's suggested protocol (Roche Diagnostics, Inc., Indianapolis, Ind.). PCR mixtures were assembled on ice and incubated at 50°C for 30 min, followed by 35 cycles of 94°C for 1 min, 55°C for 1 min, and 68°C for 1 min. The 689-bp PCR product was cloned into pCR2.1 (Invitrogen Corp., Carlsbad, Calif.). The plasmid containing the mouse glyceraldehyde-3-phosphate dehydrogenase (GAPDH) cDNA was purchased from Ambion, Inc., Austin, Tex. The nucleotide sequence of all clones was confirmed by dideoxy sequencing performed by the Nucleic Acids Core Facility at the University of Pennsylvania, Philadelphia, Pa.

Northern blot. MDBK cell monolayers (5×10^6 cells per 75-cm² flask) were infected with BVDV at 2 PFU/cell. At 1 h postinfection, the cultures were washed twice with 5 ml of 1× phosphate-buffered saline (PBS), followed by addition of 20 ml of MDBK culture medium per flask. At selected time points postinfection, the cultures were harvested by scraping the cells into the culture medium and collecting the cells by centrifugation at $500 \times g$ for 5 min at 4°C. The cell pellet was resuspended in 1 ml of 1× PBS, and the cell suspension was divided equally into separate centrifuge tubes. The cells were collected by centrifugation at $500 \times g$ for 5 min at 4°C. One set of cell pellets was frozen at −70°C

for use in immunoblot analysis. Total RNA was isolated from the cell pellets with the Biotecx RNA isolation system (Biotecx, Inc., Houston, Tex.) and quantified by spectrophotometry at 260 nm.

The RNA (15 μg) was separated by denaturing agarose gel electrophoresis on a 1% agarose gel containing 1.7% formaldehyde in 1× MOPS buffer (0.02 M morpholinopropanesulfonic acid [MOPS], 1 mM EDTA, and 5 mM sodium acetate). The RNA was transferred to positively charged nylon membrane (Hybond-N+; Amersham Pharmacia Biotech, Arlington Heights, Ill.) by Northern blotting and immobilized by UV cross-linking (Stratagene). The membranes were hybridized in Rapid Hyb solution (Amersham Parmacia Biotech, Arlington Heights, Ill.) containing 5 ng (2×10^6 cpm/ml) of ^{32}P-radiolabeled cDNA of selected ER stress marker genes per ml for 3 h at 65°C. The Northern blots were quantified by phosphorimager analysis with a Bio-Rad Personal FX phosphorimager (Bio-Rad, Inc., Hercules, Calif.). Radiolabeled probe was removed by boiling the membranes in 0.5% sodium dodecyl sulfate (SDS) for 10 min, followed by incubation for 2 min in 6× SSC (1× SSC is 0.15 M NaCl plus 0.015 M sodium citrate) at room temperature.

Immunoblot analysis. MDBK monolayers (5×10^6 cells per 75-cm² flask) were infected with BVDV at 2 PFU/cell. At selected times postinfection, the monolayers were scraped into culture medium, and the cells were collected by centrifugation at $500 \times g$ for 10 min at 4°C. The cell pellet was resuspended in 1 ml of wash buffer containing 1× PBS, 50 mM sodium fluoride, 5 mM sodium pyrophosphate, 20 mM β-glycerol phosphate, 10 mM 2-aminopurine (eIF2α kinase inhibitor), 15 mM EDTA, 1× protease inhibitor cocktail (Sigma Inc., St. Louis, Mo.; catalog number P8340), and 1× phosphatase inhibitor cocktail (Sigma Inc., St. Louis, Mo.; catalog number P2850) and collected by centrifugation at $1,000 \times g$ for 5 min at 4°C. The cells were lysed either by freeze-thaw in 0.5× radioimmunoprecipitation assay (RIPA) buffer or lysis buffer containing 100 mM Tris-HCl (pH 8.0), 20% glycerol, and 1 mM 2-β-mercaptoethanol. Both lysis buffers contained the same protease, phosphatase, and kinase inhibitors used in the wash buffer.

For analysis of phosphatase-treated proteins, 1 μl (~400 U) of lambda phosphatase (New England BioLabs, Bedford, Mass.) was added to whole-cell extracts prepared without phosphatase inhibitors and containing 100 μg of total protein and 1× lambda phosphatase buffer (50 mM Tris-HCl [pH 7.6], 2 mM MnCl₂, and 1 μg of bovine serum albumin per ml). The mixtures were incubated for 1 h at 30°C.

Equal amounts of protein extract (100 μg/lane), measured by the Bradford assay, were separated by sodium dodecyl sulfate-polyacrylamide gel electrophoresis (SDS-PAGE) on 4 to 20% polyacrylamide gradient gels. The proteins were transferred to nitrocellulose membrane by immunoblotting. The immunoblots were blocked by incubating at room temperature for 1 h in blocking buffer (1× Tris-buffered saline [TBS; 50 mM Tris-HCl, pH 7. 6, 150 mM sodium chloride], 5% nonfat dried milk, and 0.1% Tween 20). The blots were incubated with primary antibody in blocking buffer overnight with gentle rocking at 4°C.

Primary antibodies were used at the following dilutions and obtained from the indicated sources: anti-human PEK (1:1,000) was a kind gift from Ron Wek (Indiana University School of Medicine), anti-phospho-eIF2α (1:1,000) was from Research Genetics, Huntsville, Ala.; anti-eIF2α monoclonal antibody (1:1,000) (43), which recognizes total eIF2α; anti-CHOP/GADD153 (1:500) and anti-Bcl-2 (1:500) were from Santa Cruz Inc., Santa Cruz, Calif.; anti-caspase 12 (1:1,000) and antiactin monoclonal antibody (1:2,000) were from Chemicon International, Inc. Temecula, Calif.; anti-PARP (1:1,000) was from BIOMOL Research Labs, Plymouth Meeting, Pa.; and an anti-KDEL monoclonal antibody (1:1,000) (StressGen Inc., Victoria, Canada) was used to detect bovine GRP78. The blots were washed two times in blocking buffer at room temperature and incubated with horseradish peroxidase-conjugated secondary antibody (1:4,000) at room temperature for 2 h. The blots were washed two times at room temperature in 1× TBS-T (TBS containing 0.1% Tween 20) and developed with the ECL Plus chemiluminescent detection system (Amersham Pharmacia Biotech, Arlington Heights, Ill.). Densitometric analysis of scans of the immunoblots was performed to quantify the relative amounts of each protein species.

Intracellular GSH measurements. Measurement of GSH levels was performed as described previously (1). This method was adapted for MDBK cells. Briefly, MDBK cells (10^6 cells in a 35-mm-diameter dish) were scraped into medium and collected by centrifugation at $1,000 \times g$ for 10 min at 4°C. The cell pellet was washed by resuspension in ice-cold 1× PBS, and the cells were collected by centrifugation at $1,000 \times g$ for 10 min at 4°C. The cell pellet was resuspended in 80 μl of 10 mM HCl and frozen at −70°C. The cells were thawed and immediately sonicated (ultrasonicator from Heat Systems, Farmington, N.Y.) at 40% power for 40 s at 0°C. Then 20 μl of 5% 5-sulfosalicylic acid was added to the samples immediately after sonication. Cell debris was removed by centrifugation at $14,000 \times g$ for 15 min at 4°C.
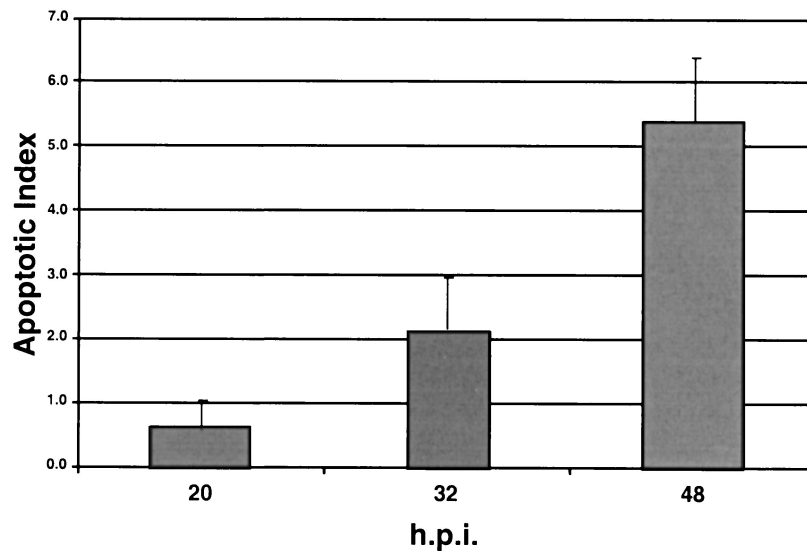
A.
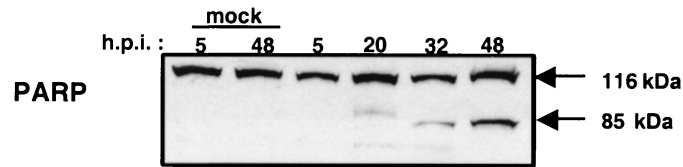
B.

FIG. 1. Infection of MDBK cells with cpBVDV causes apoptosis. (A) Immunoblot analysis during a time course of BVDV infection. Virus-induced PARP cleavage initiates at ~20 h postinfection (h.p.i.). (B) Single-stranded DNA ELISA of MDBK cells mock infected or infected with BVDV. Infections were performed in triplicate. The apoptotic index represents the change in ELISA signal relative to mock-infected samples.

The supernatant fluids were collected, and 20 μl of the cell extracts or GSH standard solution was added to reaction mixtures containing 0.1 M sodium phosphate buffer (pH 7.6), 0.24 mM NADPH, 2.5 mM EDTA, and 0.2 U of glutathione reductase per ml. GSH standard solutions containing 0 to 100 μM GSH were prepared in 0.1% 5-sulfosalicylic acid and used to generate a standard curve. The reactions were initiated by addition of 5,5′-dithiobis(2-nitrobenzoic acid) (DTNB) to a final concentration of 0.45 mM. Reduction of DTNB was measured spectrophotometrically at 405 nm at 2-min intervals for 10 min. The rate of product formation as a function of time was used to calculate the GSH levels in cell extracts by comparison to the standard curve. Protein concentrations in cell extracts were determined by the Bradford assay and used to normalize GSH levels.

Apoptosis measurements. Apoptosis of infected MDBK cells was measured by a quantitative enzyme-linked immunosorbent assay (ELISA) method according to the manufacturer's protocol (Chemicon International, Inc. Temecula, Calif.). Briefly, MDBK cells (5×10^4 per well of a 96-well tray) were mock infected or infected with BVDV at 2 PFU/cell, and the cultures were incubated for 20, 32, and 48 h. The cultures were treated with 80% methanol in 0.2× PBS (fixing solution) for 30 min at room temperature. The fixing solution was removed, and the cultures were air dried at room temperature. Then 50 μl of formamide was added to each well, and the plates were incubated for 10 min at room temperature. The plates were heated to 75°C for 10 min. The plates were cooled, and 200 μl of 3% nonfat dried milk in water (blocking solution) was added to each well and incubated for 1 h at 37°C. The blocking solution was removed, and 200 μl of a solution containing a horseradish peroxidase-conjugated antibody that

specifically binds to single-stranded DNA was added to each well, and the plates were incubated at 37°C for 1 h. The wells were washed three times with 250 μl of 1× PBS, followed by addition of 100 μl of 2,2′azino-bis/2ethylbenz-thiazoline-6-sulfonic acid diammonium salt (ABTS) developing solution. The absorbance at 405 nm was measured at 5-min intervals for 30 min to ensure that color development was linear over time. The apoptotic index was calculated by dividing the absorbance value at 405 nm for BVDV-infected cells by the absorbance value for mock-infected MDBK cells at each time point.

RESULTS

BVDV induces apoptosis of the infected cell. Infection of MDBK cells with BVDV strain NADL causes oxidative stress and leads to apoptosis of the infected cell (41). A hallmark of apoptosis is cleavage of the nuclear 116-kDa PARP (poly-[ADP-ribose] polymerase) protein to an 85-kDa inactive polypeptide (34). Inactivation of PARP through proteolytic cleavage facilitates chromosomal DNA fragmentation as part of the cellular apoptotic program (23).

Immunoblot analysis of MDBK cells infected with BVDV strain NADL at 2 PFU/cell showed PARP cleavage starting at 20 h postinfection (Fig. 1A). This time point corresponded to

the onset of cytopathic effects (data not shown) and an increase in the level of DNA fragmentation measured by an ELISA-based assay that detects the presence of single-stranded DNA in the nucleus (Fig. 1B). These results are consistent with previously published work and confirm that, under the conditions used in our experiments, BVDV strain NADL induces apoptosis of the infected cell (41).

BVDV strain NADL induces ER stress. While it is well documented that cytopathic strains of BVDV induce apoptosis, the signals that initiate the apoptotic program are not well understood. BVDV replicates in the cytoplasm of infected cells and utilizes the ER as the site of polyprotein processing and genomic replication (9, 20). During the normal course of infection, BVDV envelope glycoproteins accumulate in the ER lumen (20). Based on the premise that ER-tropic viruses induce ER stress, we examined the effects of BVDV infection on the expression of selected ER stress marker gene products.

GRP78 induction. GRP78 is a resident ER chaperone whose expression is upregulated in response to ER stress (31). To determine if GRP78 was induced by BVDV infection, Northern blot analysis was performed on total cellular RNA isolated from mock-infected or BVDV-infected MDBK cells harvested at 24 h postinfection. As a control for induction of ER stress, separate cultures of MDBK cells were treated with the pharmacological ER stress-inducing agents thapsigargin and tunicamycin. Thapsigargin induces ER stress by mobilizing calcium from the ER, while tunicamycin interferes with glycoprotein folding by blocking N-linked glycosylation in the ER.

Northern blot analysis showed that BVDV infection increased GRP78 mRNA expression by ~4-fold relative to mock-infected cells (Fig. 2A, BVDV versus mock). Treatment with thapsigargin or tunicamycin increased GRP78 mRNA levels by ~8- and ~20-fold, respectively, relative to mock-infected cells (Fig. 2A). The differential effects of BVDV infection and ER stress-inducing agents on induction of GRP78 mRNA may reflect the level of ER stress generated by each agent. Notably, the concentrations of both thapsigargin and tunicamycin were sufficient to induce apoptosis of MDBK cells within 48 h posttreatment (data not shown).

To determine the effect of BVDV infection on GRP78 protein expression, immunoblot analysis was performed on protein lysates prepared from BVDV-infected MDBK cells. MDBK cells were infected with BVDV at 2 PFU/cell, and protein lysates were prepared at 5, 15, 20, 25, and 30 h postinfection (Fig. 2B). The immunoblot shows that GRP78 levels were induced fourfold by 15 h postinfection compared to mock-infected cells (Fig. 2B, 5M and 30M) and that the level of GRP78 protein expression remained elevated compared to mock-infected cells during the course of infection. Reprobing the immunoblot with a monoclonal antibody specific for actin demonstrated that approximately equal amounts of protein were present in each lane. Virus yields measured from infected cell supernatants showed a progressive increase in the production of infectious virus that reached a plateau at 20 h postinfection These replication kinetics are consistent with single-cycle virus replication. Taken together, the results of these experiments indicate that BVDV and the ER stress-inducing agents thapsigargin and tunicamycin upregulate and/or stabilize GRP78 mRNA levels, leading to increased expression of GRP78 protein.
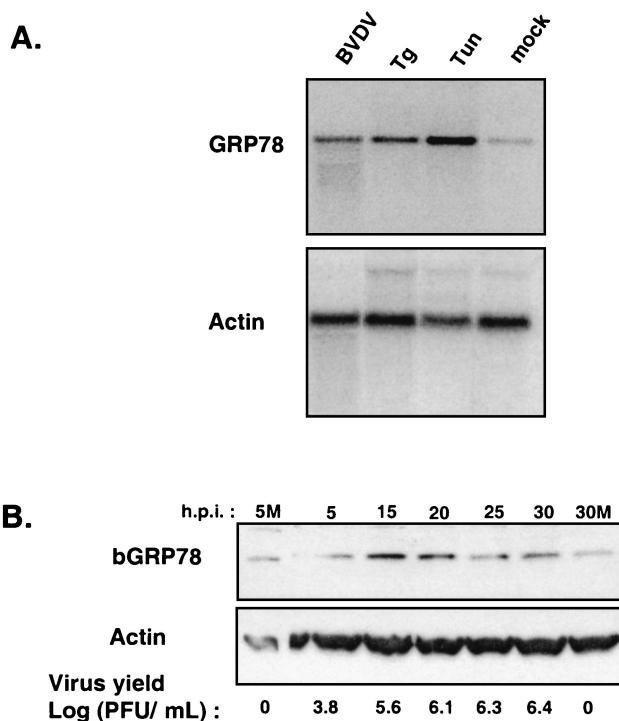

FIG. 2. Induction of GRP78 expression by BVDV infection and ER stress-inducing agents. (A) MDBK cells were infected with BVDV or treated with either 1 μg of tunicamycin (Tun) per ml or 50 nM thapsigargin (Tg) and harvested at 24 h postinfection (h.p.i.). Northern blot analysis was performed with a radiolabeled bovine GRP78 cDNA probe. The blot was stripped and rehybridized to a radiolabeled actin cDNA probe. (B) Immunoblot analysis of GRP78 protein levels during a time course of BVDV infection. MDBK cells were infected with BVDV and harvested at the indicated times. Approximately 100 μg of total cell protein from cells harvested at each time point was fractionated by SDS-PAGE on 4 to 20% polyacrylamide gels and subjected to immunoblot analysis with anti-KDEL polyclonal antibodies and monoclonal antibodies against actin. Enhanced chemiluminescence was used to visualize immune complexes. Virus yields in the culture supernatants were measured by plaque assay. 5M and 30M, 5 and 30 h post-mock infection, respectively.

PERK activation and eIF2α phosphorylation. ER stress signaling is mediated by activation of the ER transmembrane kinase PERK (17). PERK is an eIF2α kinase that exists as an inactive monomer in unstressed cells. During conditions of ER stress, PERK monomers dimerize and autophosphorylate (26). The dimeric phosphorylated form of PERK is catalytically active and able to phosphorylate its substrate, eIF2α, at serine 51. Phosphorylation of eIF2α-S51 leads to downregulation of translation initiation through a well-characterized mechanism involving inhibition of eIF2B activity (39). To determine the effect of BVDV infection on eIF2α kinase activity, the level of phospho-eIF2α-S51 in BVDV-infected MDBK cells was determined by immunoblot analysis. As a control for PERK activation, ER stress was induced in MDBK cells by treatment with 10 mM dithiothreitol (DTT). DTT disrupts protein disulfide bonds and causes accumulation of misfolded proteins in the ER lumen.

Protein extracts from MDBK cells were prepared at 24 h postinfection or 2 h post-DTT treatment, and the levels of
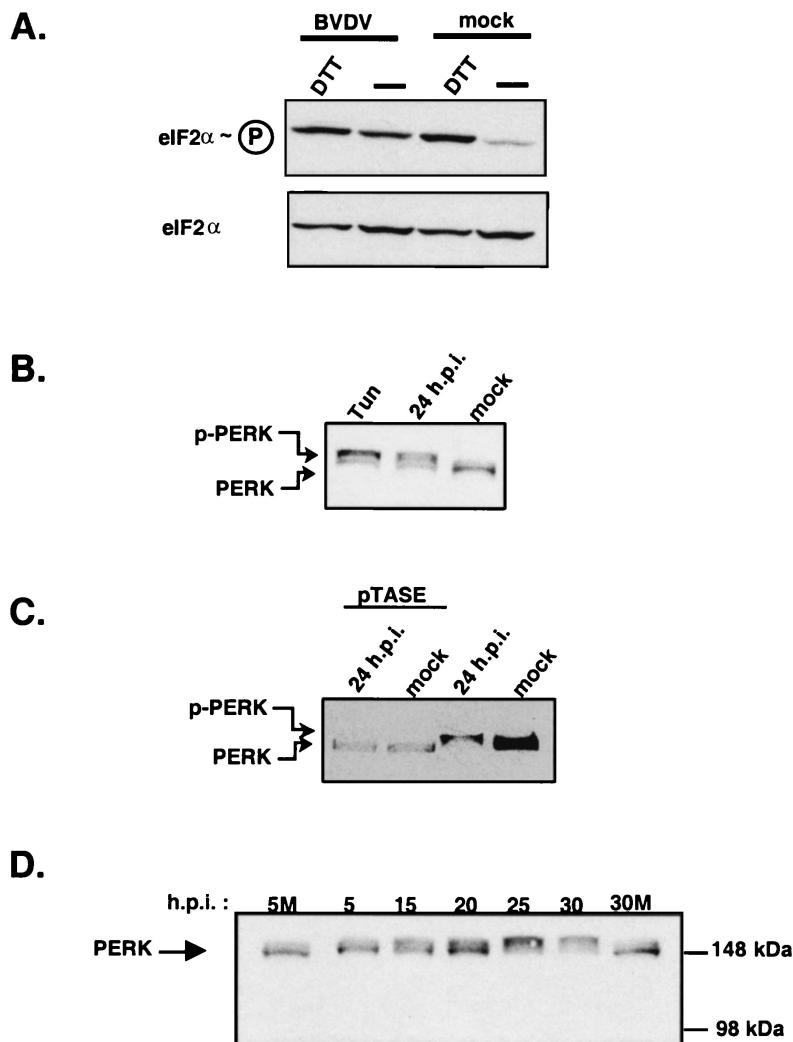
A.

B.

C.

D.

FIG. 3. BVDV infection leads to PERK activation and eIF2α-S51 phosphorylation. (A) Immunoblot analysis of total cell protein lysates prepared from BVDV-infected MDBK cells at 24 h postinfection (h.p.i.) or MDBK cells treated with 10 mM DTT for 2 h. The blot was first probed with antibodies that recognized phospho-eIF2α-S51. The blot was stripped and reprobed with a monoclonal antibody that recognizes total eIF2α. (B) Immunoblot analysis showing relative PERK mobilities from MDBK cells either mock infected, BVDV infected, or treated with 1 μg of tunicamycin (Tun) per ml for 24 h. The immunoblot was probed with an antibody specific for human PEK. (C) Lambda phosphatase (pTASE) treatment of protein lysates from mock-infected or BVDV-infected MDBK cells analyzed by immunoblotting. The positions of phosphorylated (p-PERK) and nonphosphorylated PERK are indicated. (D) Immunoblot analysis of PERK expression from mock-infected (M) or BVDV-infected MDBK cells during a time course of infection. Immunoblot analysis was performed as described for Fig. 2.

phospho-eIF2α-S51 were determined by immunoblot analysis with a phospho-eIF2α-S51-specific polyclonal antibody. The blots were stripped and reprobed with a monoclonal antibody that recognizes total eIF2α. The effect of BVDV infection and DTT treatment on eIF2α kinase activity was determined by comparing the ratio of band intensities of phospho-eIF2α-S51 and total eIF2α. The results show that BVDV infection increased the level of eIF2α-S51 phosphorylation by 15 to 20% relative to mock-infected cultures (Fig. 3A, compare lanes BVDV/− and mock/−). This level of phosphorylation is sufficient to cause growth-inhibitory effects in yeast as well as in mammalian cells (4).

Treatment of MDBK cells with DTT also increased eIF2α-S51 phosphorylation (Fig. 3A, mock/DTT). Notably, treatment of MDBK cells with DTT after infection with BVDV did not

increase the level of eIF2α phosphorylation above that with DTT treatment alone (Fig. 3, BVDV/DTT versus mock/DTT). This suggests that the effects of DTT treatment lead to maximal eIF2α kinase activity. The results show that BVDV infection activates cellular eIF2α stress-signaling pathways.

To determine if BVDV infection caused PERK activation, immunoblot analysis was performed on protein extracts prepared from BVDV-infected (24 h postinfection) or tunicamycin-treated MDBK cells (Fig. 3B). This analysis showed that PERK migrated at a higher molecular weight during SDS-PAGE in BVDV-infected and tunicamycin-treated cells than in mock-infected cells. This result is consistent with previous reports showing a slower mobility of the activated and highly phosphorylated form of PERK compared to the latent form of the kinase (17). Treatment of the protein extracts with lambda
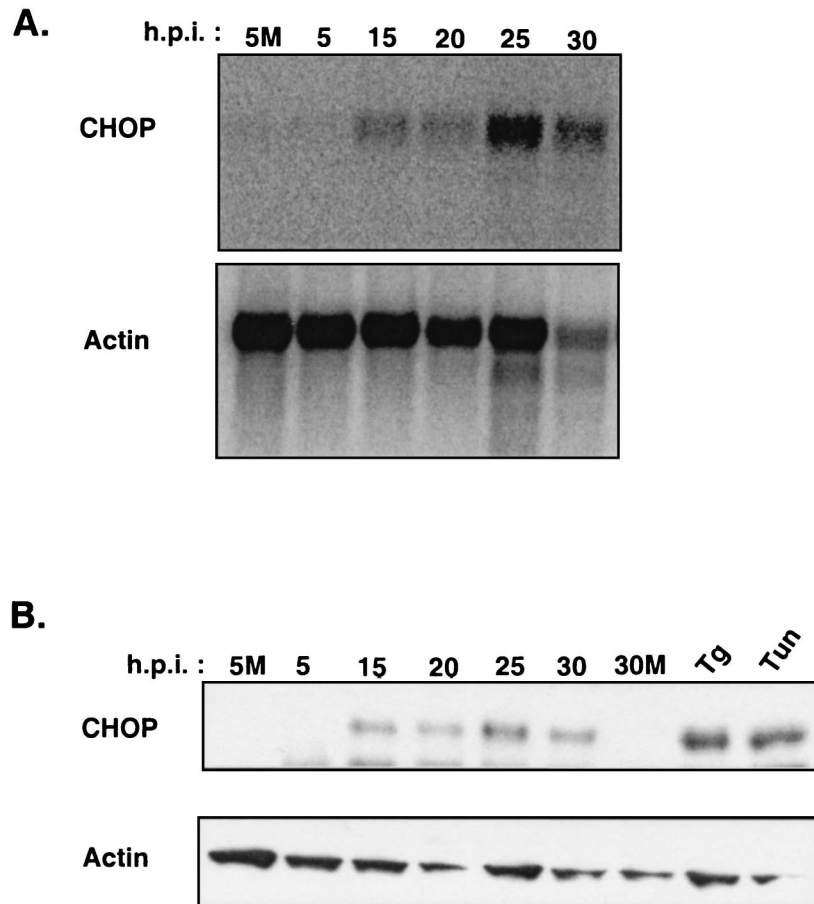
FIG. 4. Induction of GADD153/CHOP expression by BVDV infection. (A) Northern blot analysis of total mRNA from BVDV-infected MDBK cells during a time course of BVDV infection. The Northern blots were probed with a radiolabeled cDNA probe for bovine *GADD153/CHOP* or bovine actin. (B) Immunoblot analysis of 0.5× RIPA protein lysates made from MDBK cells during BVDV infection. As positive controls for CHOP induction, MDBK cells were treated with either 1 μg of tunicamycin (Tun) per ml or 50 nM thapsigargin (Tg) and harvested at 24 h posttreatment. The blots were probed with antibody specific for GADD153/CHOP protein and then stripped and reprobed with a monoclonal antibody specific for actin as described above. 5M and 30M, 5 and 30 h post-mock infection, respectively.

phosphatase prior to SDS-PAGE caused an increase in PERK mobility. PERK from phosphatase-treated extracts comigrated with PERK from mock-infected cells, suggesting that the reduced mobility of PERK in BVDV-infected or tunicamycin-treated MDBK cells was caused by phosphorylation (Fig. 3C).

Consistent with these observations, protein extracts from a time course of infection showed a progressive increase in the level of PERK phosphorylation as determined by a decrease in mobility during SDS-PAGE (Fig. 3D). Notably, a change in PERK mobility was observed within 5 h postinfection, long before the production of significant amounts of infectious virus or the appearance of any cytopathic effects. Interestingly, the highest levels of PERK phosphorylation correlated with the time of highest virion production and onset of cellular apoptosis (~25 h postinfection). Taken together, these results strongly suggest that BVDV infection causes ER stress leading to PERK activation and eIF2α phosphorylation.

CHOP/GADD153 induction. CHOP/GADD153 is a nuclear transcription factor that can form heterodimers with C/EBP proteins and negatively regulate their transcriptional activity (38). Transcriptional induction of *CHOP/GADD153* has been shown to closely parallel that of GRP78 under various ER

stress-producing conditions (15, 57). In addition, *CHOP/GADD153* induction requires PERK activation and eIF2α-S51 phosphorylation (16, 40, 57). Since BVDV infection induced GRP78 expression and increased the level of eIF2α-S51 phosphorylation, we predicted that BVDV infection would induce *CHOP/GADD153* expression.

To determine the effect of BVDV infection on *CHOP/GADD153* expression, Northern and immunoblot analysis was performed. MDBK cells were mock infected or infected with BVDV, and at 0, 5, 15, 20, 25, and 30 h postinfection, total RNA and protein lysates were prepared and analyzed by Northern and Western blotting (Fig. 4A and B). BVDV infection increased the steady-state level of *CHOP/GADD153* mRNA during the time course of infection, with peak levels of *CHOP/GADD153* mRNA (eightfold relative to that in mock-infected cells) observed at 25 h postinfection By 30 h postinfection, the signal intensity of *CHOP/GADD153* was diminished. However, the reduction in *CHOP/GADD153* signal intensity may reflect loss of mRNA during apoptosis, since actin mRNA was also reduced at this time point.

CHOP protein levels were barely detectable by immunoblot analysis in mock-infected cells (Fig. 4B, 5M and 30M) and
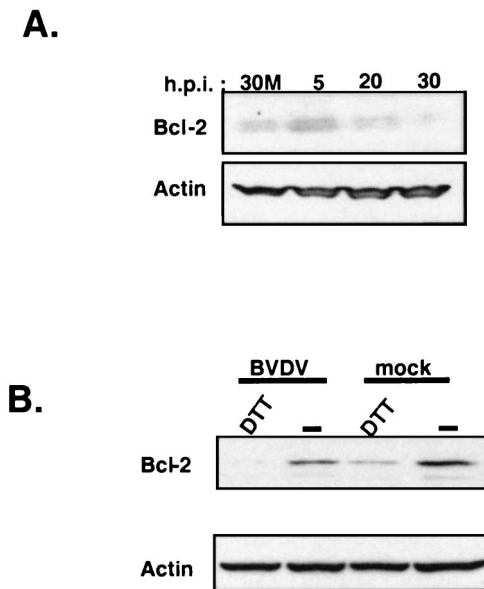
A.

B.

FIG. 5. BVDV infection and DTT treatment reduce Bcl-2 expression in MDBK cells. (A) Immunoblot analysis of protein lysates from mock-infected or BVDV-infected MDBK cells harvested at the indicated times postinfection. 30M, 30h post-mock infection. (B) Immunoblot analysis of protein lysates from BVDV-infected MDBK cells at 24 h postinfection (h.p.i.) or MDBK cells treated with 10 mM DTT for 2 h probed with anti-Bcl-2-specific antibodies; blots were stripped and reprobed with a monoclonal antibody specific for actin.

during the early time points of BVDV infection. Interestingly, CHOP protein showed an expression profile similar to that seen for *CHOP/GADD153* mRNA, with higher levels of CHOP correlating with the early phenotypic signs of cellular apoptosis at 25 h postinfection. These results show that BVDV infection induces the expression of ER stress-specific transcription factors and further support the idea that virus infection activates ER stress-signaling pathways.

Downregulation of Bcl-2. Induction of *CHOP/GADD153* has been shown to correlate with the onset of cellular apoptosis (11, 12). In addition, overexpression of CHOP caused a down-regulation of the antiapoptotic Bcl-2 protein (28). Since BVDV infection induces *CHOP/GADD153*, it was of interest to see if cellular Bcl-2 protein expression was modulated by virus infection. Immunoblot analysis of protein lysates from a time course BVDV infection showed a progressive decrease in Bcl-2 expression (Fig. 5A). These results consistently showed a significant decrease in Bcl-2 protein levels beginning at ~20 h postinfection. This result was reproducible in three different time courses of BVDV infection (data not shown). Reprobing the blots for actin demonstrated that the reduction in Bcl-2 expression was not an artifact of unequal gel loading (Fig. 5A).

Previous work has shown that overexpression of the CHOP transcription factor led to a reduction in Bcl-2 protein levels and sensitized the CHOP-overexpressing cells to apoptosis by ER stress-inducing drugs (28). Consistent with these results, we found that BVDV infection exacerbated the effects of DTT on Bcl-2 expression levels, leading to barely detectable levels of Bcl-2 protein as determined by immunoblot analysis (Fig. 5B, BVDV/DTT lane compared to mock/DTT lane). These results show that BVDV infection leads to a reduction in the steady-

state levels of Bcl-2 protein during the course of infection. Taken together, these results suggest that virus-induced depletion of cellular Bcl-2 protein may prime the infected cell for apoptosis and that virus infection sensitizes the cell to ER stress induced by pharmacological agents.

Reduction of glutathione levels. Studies performed in numerous cell systems have shown that downregulation of Bcl-2 expression leads to increased levels of intracellular ROS and depletion of intracellular glutathione (50). ROS levels also increase during BVDV infection, and this increase correlates with the onset of BVDV-induced apoptosis (41). Virus-induced apoptosis can be attenuated by addition of the phenolic antioxidant BHA (butylated hydroxyanisole) to the culture medium (41). BHA reduces ROS production and limits cytopathic effects caused by BVDV replication (41). BHA increases intracellular glutathione levels through a mechanism that up-regulates transcription of glutamate-cysteine ligase (*GCLC*). *GCLC* is the catalytic subunit of glutamate-cysteine ligase and the rate-limiting enzyme in glutathione biosynthesis (19). Since BVDV infection downregulates Bcl-2 expression and addition of BHA to the culture medium of infected cells can attenuate the virus-induced cytopathic effects, it was of interest to measure the effects of BVDV infection on *GCLC* transcription and to determine whether virus infection impacted intracellular GSH levels.

The effects of BVDV infection on *GCLC* mRNA expression were determined by Northern blot analysis of total RNA from a time course infection. In MDBK cells, two *GCLC* transcripts of 4.1 kb and 3.2 kb were detected, consistent with results found for human *GCLC* (8). The Northern blot data show that BVDV infection caused a progressive decrease in both *GCLC* transcripts (Fig. 6A). At 25 h postinfection, the level of *GCLC* mRNA was reduced by sixfold relative to that for mock-infected cells. Reprobing the Northern blot with a radiolabeled riboprobe specific for GAPDH showed relatively similar amounts of *GAPDH* mRNA in all samples, demonstrating a virus-specific reduction in *GCLC* mRNA signal.

To determine if the BVDV-induced reduction in *GCLC* mRNA levels caused a decrease in the intracellular levels of GSH, a colorimetric assay was used to measure GSH levels in MDBK cell extracts (1). The level of GSH in MDBK cell lysates during a time course infection showed a progressive decrease in intracellular GSH levels during the course of infection that correlated with the loss of *GCLC* mRNA (Fig. 6A and B).

To demonstrate that ER stress specifically affects GSH levels, cell lysates were prepared from MDBK cells subjected to treatment with various apoptosis-inducing agents. These treatments included infection with BVDV, addition of tunicamycin (1 μg/ml) to the culture medium, and UV irradiation of cells in culture. All treatments induced apoptosis of the cultured cells within 48 h (data not shown). The concentration of intracellular GSH was measured as described in Materials and Methods and normalized to the total protein concentration in the extract. The level of GSH in BVDV-infected cell lysates was reduced ninefold relative to that in mock-infected-cell extracts (Fig. 6C). Similarly, tunicamycin treatment caused a threefold reduction in GSH levels. In contrast, the GSH level in UV-treated cells was similar to that of mock-infected cell lysates. These results suggest that ER stress induced by BVDV infec-
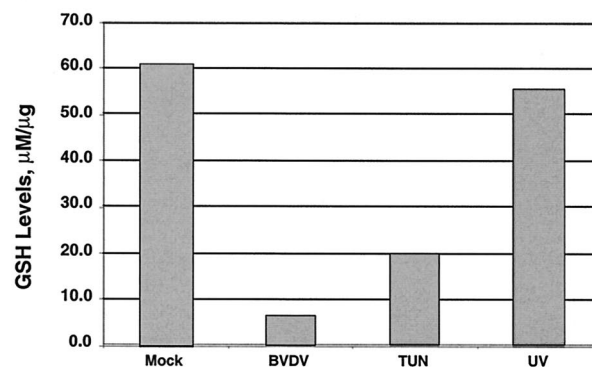
A.
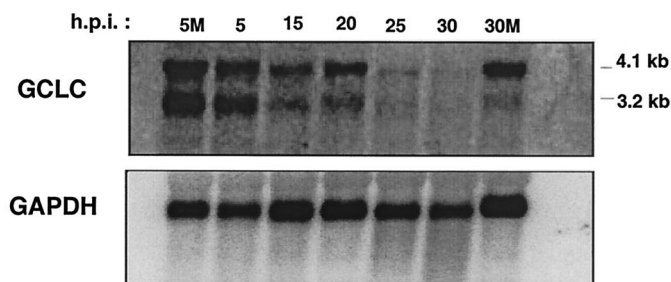
B.
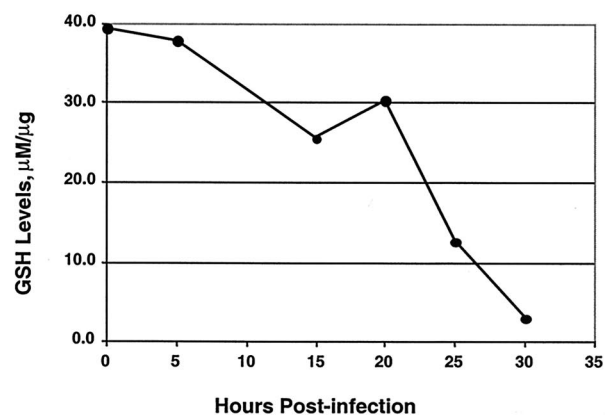
C.

FIG. 6. BVDV infection and tunicamycin treatment decrease intracellular GSH levels in MDBK cells. (A) Northern blot analysis of BVDV-infected MDBK cells harvested at the indicated times postinfection and probed with a radiolabeled cDNA probe from the human *GCLC* gene. The Northern blots were stripped and probed with a radiolabeled RNA probe specific for the mouse *GAPDH* gene. 5M and 30M, 5 and 30 h post-mock infection, respectively. (B) Intracellular levels of GSH were measured in BVDV-infected MDBK cell lysates. The GSH levels were normalized to total protein content in the cell lysates. (C) GSH levels were measured in mock-infected or BVDV-infected MDBK cells harvested at 24 h postinfection (h.p.i.). In separate cultures, MDBK cells were treated with 1 μg of tunicamycin (TUN) or irradiated with 40 μJ of UV light (218 nm). GSH levels were normalized to total protein content in the cell extracts.

tion or by tunicamycin treatment leads to a reduction in intracellular GSH levels. UV treatment, which does not induce ER stress, had little effect on GSH levels. Taken together, these results suggest that BVDV infection causes oxidative stress by reducing intracellular GSH levels through a mechanism involving downregulation of *GCLC* gene expression.

Activation of caspase 12. A hallmark of ER stress-induced apoptosis is the activation of caspase 12, an ER membrane-associated cysteine protease that is activated by ER stress-inducing agents (33, 54). Since BVDV infection appears to induce ER stress and lower GSH levels, it was of interest to determine if BVDV infection could induce caspase 12 expression. Immunoblot analysis of protein lysates from a time course infection showed that BVDV infection induced caspase 12 expression (Fig. 7A). In MDBK cells, caspase 12 was undetectable or barely detectable at 0, 5, 10, 15, or 20 h postinfection or in mock-infected cells. At 25 h postinfection, caspase 12 expression was induced coincident with the onset of apoptosis (Fig. 7A).

As a control for ER stress-induced caspase 12 expression, MDBK cells were treated with tunicamycin at levels that induced apoptosis within 48 h. In addition, MDBK cells were either irradiated with UV light or treated with etoposide to induce apopto-

sis by non-ER-stress-dependent pathways. Apoptosis of MDBK cells was confirmed by terminal deoxynucleotidyltransferase-mediated dUTP-biotin nick-end labeling (TUNEL) assay and the appearance of altered nuclear morphology following 4′,6′-diamidino-2-phenylindole (DAPI) staining and immunofluorescence microscopy (data not shown).

Immunoblot analysis showed that of the three treatments, only tunicamycin treatment induced caspase 12 protein expression (Fig. 7B, lower band). These results indicate that ER stress caused by BVDV infection or a pharmacological agent induces caspase 12 expression in MDBK cells, consistent with the caspase 12 expression profile seen in human 293T cells following treatment with ER stress-inducing drugs (36). Induction of caspase 12 by BVDV infection strongly suggests that virus-induced ER stress activates the apoptotic program in infected cells and that ER stress signaling contributes significantly to the cytopathogenesis associated with this strain of BVDV.

DISCUSSION

Viruses that utilize the ER as the primary site of replication must contend with the ER stress response and ER stress sig-
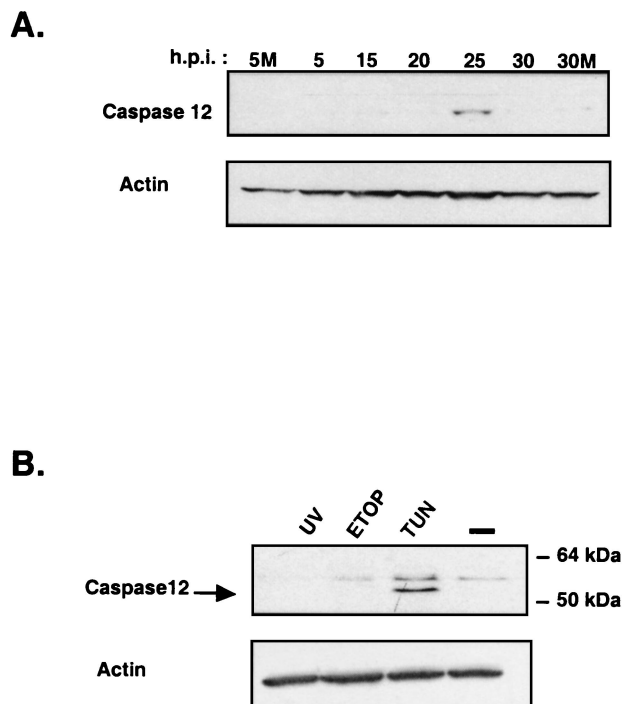
A.

B.

FIG. 7. Induction of caspase 12 expression by BVDV infection or treatment with tunicamycin. (A) Immunoblot analysis of protein lysates from BVDV-infected MDBK cells harvested during a time course infection. Blots were probed with polyclonal antibodies specific for caspase 12. 5M and 30M, 5 and 30 h post-mock infection, respectively. (B) Immunoblot analysis of protein lysates from MDBK cells irradiated with 40 μJ of UV (218 nm) or treated with 100 μM etoposide (ETOP) or 1 μg of tunicamycin (TUN) per ml for 24 h. Blots were initially probed for caspase 12, then stripped and reprobed with a monoclonal antibody specific for actin.
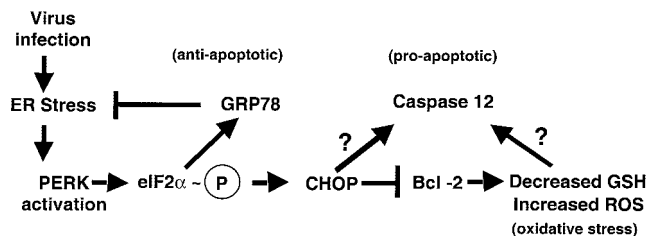

FIG. 8. Model of BVDV-induced ER stress. Virus-induced ER stress activates both pro- and antiapoptotic signaling. While induction of GRP78 is required to maintain cellular homeostasis in response to ER stress and overexpression of GRP78 protects cells from ER stress-induced apoptosis, extreme or prolonged ER stress may push cells past a certain stress threshold that activates the cellular apoptotic program. High-level PERK activation and eIF2α phosphorylation (circled P) induce CHOP expression, which may lead to reductions in Bcl-2 levels. Reduction in Bcl-2 expression correlates with changes in cellular redox status and the production of reactive oxygen species (ROS). BVDV-induced decreases in Bcl-2 levels correspond to large reductions in intracellular glutathione levels. As infection proceeds, increased cellular stress levels activate caspase 12 and the cellular apoptotic program. The molecular signals responsible for activating caspase 12 are currently unknown.

naling in order to maximize replication efficiency. In this report, we show that a cytopathic strain of BVDV induces an ER stress response. The ER stress response in BVDV-infected cells was defined by specific marker gene products whose level of expression was determined by Northern and immunoblot analysis. The results from this study are consistent with a model in which virus infection causes a high and/or prolonged level of ER stress that results in activation of an ER stress-specific apoptotic pathway(s). A summary of the virus-induced ER stress-signaling pathway suggested by this study is shown in Fig. 8. Note that this pathway shows ER stress inducing both pro- and antiapoptotic activities.

BVDV induces an ER stress response. (i) GRP78 and CHOP/GADD153. BVDV infection induced expression of GRP78 and CHOP/GADD153. GRP78 is an ER-resident chaperone protein that facilitates protein folding in the ER, while CHOP/GADD153 is a transcription factor that can heterodimerize with C/EBP transcription factor family members and negatively regulate their activity (31, 38). Upregulation of *CHOP/GADD153* mRNA has been shown to closely parallel that of GRP78 under various ER stress-producing conditions, making induction of these two gene products markers of ER stress signaling (15). In addition, while overexpression of GRP78 protects cells from ER stress-induced apoptosis, overexpression of *CHOP/GADD153* leads to cell cycle arrest and

apoptosis through mechanisms that may involve downregulation of Bcl-2 (discussed below) (11, 12, 31). Thus, ER stress signaling induces both pro- and antiapoptotic activities and suggests that cytopathic BVDV infection generates a level of ER stress signaling that activates cellular apoptotic pathways.

(ii) PERK activation. Induction of *CHOP/GADD153* in response to ER stress requires PERK-mediated eIF2α phosphorylation (15, 40). Immunoblot analysis with phospho-eIF2α-S51-specific antibodies showed that BVDV caused a marked increase in eIF2α phosphorylation, consistent with activation of an eIF2α kinase. PERK is an ER transmembrane eIF2α kinase with an ER-luminal regulatory domain and a cytoplasmic kinase domain (17). The current model for PERK regulation proposes that, under normal conditions, PERK is held in a latent, monomeric form by ER chaperone proteins GRP78 and GRP94 bound to the ER-luminal domain of PERK. During ER stress, as unfolded or aggregated proteins accumulate in the lumen, GRP78 and GRP94 release from the kinase to assist in protein folding. Under these stress conditions PERK is then able to dimerize and autophosphorylate (26). The phosphorylated form of PERK is catalytically active and able to phosphorylate eIF2α (27).

Recent work has shown that PERK is a key mediator of ER stress signaling (25, 40). BVDV infection of MDBK cells led to a rapid induction of PERK activity, as seen by the increase in PERK autophosphorylation over the course of BVDV infection (Fig. 3D). Notably, PERK phosphorylation was maximal during peak times of virion production, starting at ~15 h postinfection, suggesting that the level of ER stress signaling increased as synthesis of viral gene products and production of new virions reached a maximum (Fig. 3D). The increased level of PERK phosphorylation correlated with the onset of apoptosis, suggesting that the level of BVDV-induced PERK phosphorylation at late time points during infection crosses a "threshold" level of ER stress signaling that may shift the ER stress equilibrium towards apoptosis.

Double-stranded RNA produced during the course of

BVDV infection might be predicted to activate the interferon antiviral response and the interferon-inducible kinase PKR. Presently, however, the role of the innate cellular response to BVDV infection is unclear (2, 42). While a direct connection between the interferon-induced antiviral response and ER stress signaling has not been established, a recent study has linked control of intracellular GSH levels with phosphorylation of eIF2α (47). This suggests that cross talk between ER stress signaling and interferon antiviral pathways could converge at the level of eIF2α kinase activation. PKR is another member of the eIF2α kinase family that can inhibit virus proliferation by phosphorylating eIF2α (13). While it is possible that BVDV-activated PKR contributes to the phosphorylation of eIF2α, the role of PKR activation in BVDV-induced apoptosis is unknown. We are currently looking at the connections between ER stress signaling and the innate immune response.

Downregulation of Bcl-2 and loss of GSH. PERK-mediated signaling and activation of CHOP/GADD153 expression contribute to initiation of the apoptotic cascade through downregulation of the antiapoptotic gene *Bcl-2*. Overexpression of CHOP/GADD153 has been shown to downregulate Bcl-2 and sensitize the cell to ER stress (28). Interestingly, dengue virus- and Japanese encephalitis virus-induced apoptosis of BHK-21 cells can be rescued by overexpression of Bcl-2, changing the outcome of virus infection from cytopathic to chronic (44, 45). Our results shows that BVDV-induced apoptosis also correlates with downregulation of Bcl-2. These results suggest that ER stress-induced regulation of Bcl-2 expression can influence the cellular pathogenesis of ER-tropic virus infection and likely contributes to BVDV-induced apoptosis.

Downregulation of Bcl-2 has been shown to decrease intracellular GSH levels and increase ROS, thereby enhancing the cells' susceptibility to oxidant injury (28, 50). Consistent with this observation, BVDV infection led to a reduction in *GCLC* mRNA, the catalytic subunit of glutamate-cysteine ligase and the rate-limiting enzyme in glutathione biosynthesis (8). Concomitant with the loss of *GCLC* mRNA was a dramatic decrease in intracellular GSH levels which corresponded with the phenotypic onset of apoptosis seen at 20 to 25 h postinfection (Fig. 6B).

Caspase 12 activation. Activation of caspase 12 may represent the final stage in ER stress-induced apoptosis. Caspase 12 is an ER membrane-associated cysteine protease that is induced and activated by ER stress (33, 36, 54). It has been suggested that caspase 12 is a key mediator of ER stress-induced apoptosis and is required for recruiting other cytosolic caspases to the ER membrane to propagate the apoptotic signal (36).

Our results show that during BVDV infection, induction of caspase 12 expression correlates with the onset of apoptosis at ~25 h postinfection. Presently, only ER stress has been shown to induce caspase 12 activity (33). Taken together, our observations strongly suggest that BVDV infection activates ER stress signaling pathways that initiate an apoptotic cascade involving downregulation of Bcl-2 expression, changes in redox regulation, and induction of caspase 12. These results define some of the molecular connections between virus-generated ER stress signaling and activation of downstream pathways leading to apoptosis.

Initiation of BVDV-induced ER stress. ER stress is typically induced by alteration in calcium stores or accumulation of unfolded or unassembled proteins in the ER lumen. BVDV and other flaviviruses such as HCV encode viral envelope glycoproteins that accumulate to high levels in the ER lumen (5, 6, 10, 20). Moreover, HCV envelope proteins exist as high-molecular-weight aggregates that are not recognized by conformation-specific antibodies, suggesting that they exist in nonnative conformations (3). Overexpression of HCV glycoproteins activates *grp78* and *grp94* promoters in transient gene expression assays, consistent with the induction of an ER stress response (24). In addition, expression of HCV proteins in a hepatoma cell line (HepG2) induces apoptosis (21). Therefore, it is tempting to speculate that BVDV-induced ER stress is mediated through signals that emanate from the ER lumen and are caused by the presence of unfolded or unassembled viral glycoproteins.

While accumulation of unfolded proteins in the ER lumen is the most plausible explanation for induction of ER stress, isogenic cytopathic and noncytopathic strains of BVDV have been isolated that replicate with equal efficiencies and produce similar numbers of infectious virions yet differ in their ability to cause cytopathic effects (30). How do noncytopathic strains of BVDV replicate without inducing lethal ER stress?

Studies of isogenic strains of BVDV have demonstrated that cytopathogenicity correlates with increased cleavage at the NS2-3 locus and production of NS3 protein (29, 48). NS3 is a nonstructural protein that likely associates with the cytosolic side of the ER and is involved in polyprotein cleavage (51–53). An ER-resident integral membrane protein, Jiv, which contains a DnaJ homology region, modulates NS2-3 cleavage during infection. Overexpression of Jiv increases NS2-3 cleavage efficiency during replication of noncytopathic strains of BVDV and promotes virus-induced cytopathic effects (37). While NS3 production has been linked to cytopathogenicity, a recent study has identified point mutations in NS4b that can suppress cytopathic effects while maintaining wild-type levels of virus replication and NS2-3 cleavage (35). This second-site mutation in NS4b uncouples production of NS3 from cytopathic effects and suggests that the mechanism of virus-induced cytopathogenicity is more complex than was previously thought. More importantly, these studies suggest that initiation of ER stress signaling may involve more than just intraluminal accumulation of unfolded or unassembled viral proteins.

Assembly of the viral replicase on the cytosolic face of the ER may contribute to activation of ER stress signaling. The nonstructural proteins (NS2, NS3, NS4a, NS4b, NS5a, and NS5b) of HCV and Kunjin virus localize to the ER and modified ER-like membrane structures that are readily visible by electron microscopy (32, 51). Moreover, the NS4a protein of HCV directs NS3 to the ER, increases NS3 protein stability, and facilitates NS3-dependent *trans*-cleavage of NS4-5 (52). Transient expression of HCV NS5a alters intracellular calcium levels, induces oxidative stress, and activates STAT-3 and NF-κB (14). Thus, changes in ER function associated with assembly of the viral replicase may lead to activation of ER stress signaling. Perhaps cytopathic strains of BVDV produce an altered replicase as the result of increased NS2-3 cleavage, which can induce ER stress signaling. This altered replicase, coupled with the accumulation of viral glycoproteins in the ER

lumen, may induce lethal levels of ER stress signaling, leading to apoptosis of the infected cell.

We have shown that a cytopathic strain of BVDV induces ER stress and leads to apoptosis of the infected cell. In support of our work, a recent study has shown that apoptosis induced by Japanese encephalitis virus correlates with induction of an ER stress response (44). While this extreme phenotype demonstrates the importance of ER stress signaling in the cellular pathogenesis of ER-tropic viruses, the consequences of chronic ER stress signaling during infection with noncytopathic ER-tropic viruses, such as HBV and HCV, have not been fully realized. Cells undergoing ER stress have been shown to be more susceptible to oxidative damage and exhibit reduced DNA repair capacity (7). Thus, chronic ER stress during persistent viral infection could sensitize infected cells to genotoxic insults and oxidative damage, which could ultimately lead to oncogenic transformation. The effects of noncytopathic BVDV infection on the induction of ER stress signaling are currently under study.

ACKNOWLEDGMENTS

REFERENCES

1. **Allen, S., J. M. Shea, T. Felmet, J. Gadra, and P. F. Dehn.** 2001. A kinetic microassay for glutathione in cells plated on 96-well microtiter plates. Methods Cell Sci. **22:**305–312.
2. **Charleston, B., L. S. Brackenbury, B. V. Carr, M. D. Fray, J. C. Hope, C. J. Howard, and W. I. Morrison.** 2002. Alpha/beta and gamma interferons are induced by infection with noncytopathic bovine viral diarrhea virus in vivo. J. Virol. **76:**923–927.
3. **Choukhi, A., S. Ung, C. Wychowski, and J. Dubuisson.** 1998. Involvement of endoplasmic reticulum chaperones in the folding of hepatitis C virus glycoproteins. J. Virol. **72:**3851–3858.
4. **Clemens, M. J.** 1996. Protein kinases that phosphorylate eIF2α and eIF2b and their role in eukaryotic cell translational control, p. 139–172. *In* J. W. B. Hershey, M. B. Mathews, and N. Sonenberg (ed.), Translational control. Cold Spring Harbor Laboratory Press, Cold Spring Harbor, N.Y.
5. **Cocquerel, L., S. Duvet, J. C. Meunier, A. Pillez, R. Cacan, C. Wychowski, and J. Dubuisson.** 1999. The transmembrane domain of hepatitis C virus glycoprotein E1 is a signal for static retention in the endoplasmic reticulum. J. Virol. **73:**2641–2649.
6. **Cocquerel, L., J. Meunier, A. Pillez, C. Wychowski, and J. Dubuisson.** 1998. A retention signal necessary and sufficient for endoplasmic reticulum localization maps to the transmembrane domain of hepatitis C virus glycoprotein E2. J. Virol. **72:**2183–2191.
7. **Collins, A. R.** 1999. Oxidative DNA damage, antioxidants, and cancer. BioEssays **21:**238–246.
8. **Dahl, E. L., and R. T. Mulcahy.** 2001. Cell-type specific differences in glutamate cysteine ligase transcriptional regulation demonstrate independent subunit control. Toxicol. Sci. **61:**265–272.
9. **Donis, R. O.** 1995. Molecular biology of bovine viral diarrhea virus and its interactions with the host. Vet. Clin. N. Am. Food Anim. Practice **11:**393–423.
10. **Duvet, S., L. Cocquerel, A. Pillez, R. Cacan, A. Verbert, D. Moradpour, C. Wychowski, and J. Dubuisson.** 1999. Hepatitis C virus glycoprotein complex localization in the endoplasmic reticulum involves a determinant for retention and not retrieval. J. Biol. Chem. **273:**32088–32095.
11. **Eymin, B., L. Dubrez, M. Allouche, and E. Solary.** 1997. Increased gadd1 53 messenger RNA level is associated with apoptosis in human leukemic cells treated with etoposide. Cancer Res. **57:**686–695.
12. **Friedman, A. D.** 1996. GADD153/CHOP, a DNA damage-inducible protein, reduced CAAT/enhancer binding protein activities and increased apoptosis in 32D c13 myeloid cells. Cancer Res. **56:**3250–3256.
13. **Gale, J., and M. G. Katze.** 1998. Molecular mechanisms of interferon resistance mediated by viral-directed inhibition of PKR, the interferon-induced protein kinase. Pharm. Ther. **78:**29–46.
14. **Gong, G., G. Waris, R. Tanveer, and A. Siddiqui.** 2001. Human hepatitis C virus NS5A protein alters intracellular calcium levels, induces oxidative stress, and activates STAT-3 and NF-κB. Proc. Natl. Acad. Sci. USA **98:**9599–9604.
15. **Harding, H. P., I. Novoa, Y. Zhang, H. Zeng, R. C. Wek, M. Schapira, and D. Ron.** 2000. Regulated translation initiation controls stress-induced gene expression in mammalian cells. Mol. Cell **6:**1099–1108.
16. **Harding, H. P., Y. Zhang, A. Bertoletti, H. Zeng, and D. Ron.** 2000. Perk is essential for translational regulation and cell survival during the unfolded protein response. Mol. Cell **5:**897–904.
17. **Harding, H. P., Y. Zhang, and D. Ron.** 1999. Protein translation and folding are coupled by an endoplasmic-reticulum-resident kinase. Nature **397:**271–274.
18. **Hoff, H. S., and R. O. Donis.** 1997. Induction of apoptosis and cleavage of poly(ADP-ribose) polymerase by cytopathic bovine viral diarrhea virus infection. Virus Res. **49:**101–113.
19. **Huang, Z. A., H. Yang, C. Chen, Z. Zeng, and S. C. Lu.** 2000. Inducers of gamma-glutamylcysteine synthetase and their effects on glutathione synthetase expression. Biochim. Biophys. Acta **1493:**48–55.
20. **Jordan, R., O. Nikolaeva, L. Wang, B. Conyers, A. Mehta, T. M. Block, and R. A. Dwek.** 2002. Inhibition of host ER glucosidase activity prevents Golgi processing of virion-associated bovine viral diarrhea virus E2 glycoproteins and reduces infectivity of secreted virions. Virology **295:**10–19.
21. **Kalkeri, G., N. Khalap, R. F. Garry, C. D. Fermin, and D. Srikanta.** 2001. Hepatitis C virus protein expression induces apoptosis in HepG2 cells. Virology **282:**26–37.
22. **Kaufman, R. J.** 1999. Stress signaling from the lumen of the endoplasmic retiuclum: coordination of gene transcriptional and translational controls. Genes Dev. **13:**1211–1233.
23. **Lazebnik, Y. A., S. H. Kaufmann, S. Desnoyers, G. G. Poirier, and W. C. Earnshaw.** 1994. Cleavage of poly(ADP-ribose) polymerase by a proteinase with properties like ICE. Nature **371:**346–347.
24. **Liberman, E., Y. Fong, M. J. Selby, Q. Choo, L. Cousens, M. Houghton, and T. S. B. Yen.** 1999. Activation of the grp78 and grp94 promoters by hepatitis C virus E2 envelope protein. J. Virol. **73:**3718–3722.
25. **Liu, C. Y., M. Schroder, and R. J. Kaufman.** 2000. Ligand-independent dimerization activates the stress response kinases IRE1 and PERK in the lumen of the endoplasmic reticulum. J. Biol. Chem. **275:**24881–24885.
26. **Ma, K., K. M. Vattern, and R. C. Wek.** 2002. Dimerization and release of molecular chaperone inhibition facilitate activation of eukaryotic initiation factor-2 (eIF2) kinase in response to endoplasmic reticulum stress. J. Biol. Chem. **277:**18728–18735.
27. **Ma, Y., and L. M. Hendershot.** 2001. The unfolding tale of the unfolded protein response. Cell **107:**827–830.
28. **McCullough, K. D., J. L. Martindale, L. Klotz, T. Aw, and N. J. Holbrook.** 2000. Gadd153 sensitizes cells to endoplasmic reticulum stress by downregulating bcl2 and perturbing the cellular redox state. Mol. Cell. Biol. **21:**1249–1259.
29. **Mendez, E., N. Ruggel, M. S. Collett, and C. M. Rice.** 1998. Infectious bovine viral diarrhea virus (strain NADL) RNA from stable cDNA clones: a cellualr insert determines NS3 production and viral cytopathogenicity. J. Virol. **72:**4737–4745.
30. **Meyers, G., and H. Thiel.** 1996. Molecular characterization of pestiviruses. Adv. Virus Res. **47:**53–119.
31. **Morris, J. A., A. J. Dorner, C. A. Edwards, L. M. Hendershot, and R. J. Kaufman.** 1997. Immunoglobulin binding protein (BiP) function is required to protect cells from endoplasmic reticulum stress but is not required for the secretion of selective proteins. J. Biol. Chem. **272:**4327–4334.
32. **Mottola, G., G. Cardinali, A. Ceccacci, C. Trozzi, L. Bartholomew, M. Rosaria, E. Pedrazzini, S. Bonatti, and G. Migliaccio.** 2001. Hepatitis C virus nonstructural proteins are localized in a modified endoplasmic reticulum of cells expressing viral subgenomic replicons. Virology **293:**31–43.
33. **Nakagawa, T., H. Zhu, N. Morishima, E. Li, J. Xu, B. A. Yankner, and J. Yuan.** 2000. Caspase-12 mediates endoplasmic reticulum-specific apoptosis and cytotoxicity by amyloid-beta. Nature **403:**98–103.
34. **Nicholson, D. W., A. Ali, N. A. Thornberry, J. P. Vaillancourt, C. K. Ding, M. Gallant, Y. Gareau, P. R. Griffin, M. Labelle, and Y. A. Lazebnik.** 1995. Identification and inhibition of the ICE/CED-3 protease necessary for mammalian apoptosis. Nature **376:**37–43.
35. **Qu, L., L. K. McMullan, and C. M. Rice.** 2001. Isolation and characterization of noncytopathic pestivirus mutants reveals a role for nonstructural protein NS4B in viral cytopathogenicity. J. Virol. **75:**10651–10662.
36. **Rao, R. V., E. Hermel, S. Castro-Obregon, G. del Rio, L. M. Ellerby, H. M. Ellerby, and D. E. Bredesen.** 2001. Coupling endoplasmic reticulum stress to the cell death program. J. Biol. Chem. **276:**33869–33874.
37. **Rinck, G., C. Birghan, T. Harada, G. Meyers, H. Thiel, and N. Tautz.** 2001. A cellular J-domain protein modulates polyprotein processing and cytopathogenicity of a pestivirus. J. Virol. **75:**9470–9482.
38. **Ron, D., and J. F. Habener.** 1992. CHOP, a novel developmentally regulated nuclear protein that dimerizes with transcription factors C/EBP and LAP

and functions as a dominant-negative inhibitor of gene transcription. Genes Dev. **6:**439–453.

39. **Rowlands, A. G., R. Panniers, and E. C. Henshaw.** 1988. The catalytic mechanism of guanine nucleotide exchange factor action and competitive inhibition by phosphorylated eukaryotic initiation factor 2. J. Biol. Chem. **263:**5526–5533.

40. **Scheuner, D., B. Song, E. McEwen, C. Liu, R. Laybutt, P. Gillespie, T. Saunders, S. Bonner-Weir, and R. J. Kaufman.** 2001. Translational control is required for the unfolded protein response and in vivo glucose homeostasis. Mol. Cell **7:**1165–1176.

41. **Schweizer, M., and E. Peterhans.** 1999. Oxidative stress in cells infected with bovine viral diarrhea virus: a crucial step in the induction of apoptosis. J. Gen. Virol. **80:**1147–1155.

42. **Schweizer, M., and E. Peterhans.** 2001. Noncytopathic bovine viral diarrhea virus inhibits double-stranded RNA-induced apoptosis and interferon synthesis. J. Virol. **75:**4692–4698.

43. **Scorsone, K. A., R. Panniers, A. G. Rowlands, and E. C. Henshaw.** 1987. Phosphorylation of eukaryotic initiation factor 2 during physiological stresses which affect protein synthesis. J. Biol. Chem. **262:**14538–14543.

44. **Su, H., C. Liao, and Y. Li.** 2002. Japanese encephalitis virus infection initiates endoplasmic reticulum stress and an unfolded protein response. J. Virol. **76:**4162–4171.

45. **Su, H., Y. Lin, H. Yu, C. Tsao, L. Chen, Y. Liu, and C. Liao.** 2001. The effect of human bcl-2 and bcl-X genes on dengue virus-induced apoptosis in cultured cells. Virology **282:**141–153.

46. **Sullivan, D. G., and R. K. Akkina.** 1995. A nested polymerase chain reaction assay to differentiate pestiviruses. Virus Res. **38:**231–239.

47. **Tan, S., N. Somia, P. Maher, and D. Schubert.** 2001. Regulation of antioxidant metabolism by translation initiation factor 2α. J. Cell Biol. **152:**997–1006.

48. **Tautz, N., G. Meyers, R. Stark, E. Dubovi, and H. Thiel.** 1996. Cytopathogenicity of a pestivirus correlates with a 27-nucleotide insertion. J. Virol. **70:**7851–7858.

49. **Vassilev, V. B., M. S. Collett, and R. O. Donis.** 1997. Authentic and chimeric full-length genomic cDNA clones of bovine viral diarrhea virus that yield infectious transcripts. J. Virol. **71:**471–478.

50. **Voehringer, D. W., and R. E. Meyn.** 2000. Redox aspects of Bcl-2 function. Antioxidants Redox Signaling **2:**537–550.

51. **Westaway, E. G., J. M. Mackenzie, M. T. Kenney, M. K. Jones, and A. A. Khromykh.** 1997. Ultrastructure of Kunjin virus-infected cells: colocalization of NS1 and NS3 with double-stranded RNA, and of NS2B with NS3, in virus-induced membrane structures. J. Virol. **71:**6650–6661.

52. **Wolk, B., D. Sansonno, H. G. Krausslich, F. Dammacco, C. M. Rice, H. E. Blum, and D. Moradpour.** 2000. Subcellular localization, stability, and transcleavage competence of the hepatitis C virus NS3-NS4A complex expressed in tetracycline-regulated cell lines. J. Virol. **74:**2293–2304.

53. **Xu, J., E. Mendez, P. Caron, C. H. Lin, M. A. Murcko, M. S. Collett, and C. M. Rice.** 1997. Bovine viral diarrhea virus NS3 serine proteinase: polyprotein cleavage sites, cofactor requirements, and molecular model of an enzyme essential for pestivirus replication. J. Virol. **71:**5312–5322.

54. **Yoneda, T., K. Imaizumi, K. Oono, D. Yui, F. Gomi, T. Katayama, and M. Tohyama.** 2001. Activation of caspase-12, an endoplastic reticulum (ER) resident caspase, through tumor necrosis factor receptor-associated factor 2-dependent mechanism in response to the ER stress. J. Biol. Chem. **276:** 13935–13940.

55. **Zhan, Q., K. A. Lord, I. J. Alamo, M. C. Hollander, F. Carrier, D. Ron, K. W. Kohn, B. Hoffman, D. A. Liebermann, and A. J. J. Fornace.** 1994. The *gadd* and *MyD* genes define a novel set of mammalian genes encoding acidic proteins that synergistically suppress cell growth. Mol. Cell. Biol. **14:**2361–2371.

56. **Zhang, G., S. Aldridge, M. C. Clark, and J. McCauley.** 1996. Cell death induced by cytopathic bovine viral diarrhoea virus is mediated by apoptosis. J. Gen. Virol. **77:**1677–1681.

57. **Zinszner, H., M. Kuroda, X. Wang, N. Batchvarova, R. T. Lightfoot, H. Remotti, J. L. Stevens, and D. Ron.** 1998. CHOP is implicated in programmed cell death in response to impaired function of the endoplasmic reticulum. Genes Dev. **12:**982–995.